Paper

Temperature dependence of polarization mode dispersion in tight-buffered optical fibers

Krzysztof Borzycki

Abstract—Experiments and theoretical analysis of influence of temperature on polarization mode dispersion (PMD) in single mode optical fibers and cables are presented. Forces generated by contracting buffer create optical birefringence and increase fiber PMD at low temperatures. Single mode fiber (SMF) in 0.9 mm polymeric tight-buffer can exhibit an extra component of PMD exceeding 0.3 ps/$\sqrt{\text{km}}$ in such conditions. On the other hand, tight-buffered spun nonzero dispersion-shifted fibers (NZDSF) and optical units with stranded single mode fibers have showed good stability of PMD over wide range of temperatures. This is due to presence of circular strain in the core, blocking accumulation of mechanically induced birefringence.

Keywords— single mode optical fiber, polarization mode dispersion, birefringence, environmental testing, tight-buffered fiber, optical fiber cable, optical ground wire, temperature cycling, polymer.

1. Introduction

Polarization mode dispersion (PMD) is detrimental to high speed optical fiber transmission, thus attracting considerable interest. This phenomenon results from imperfections in fiber geometry and external mechanical disturbances: pressure, bending, twisting, etc. While improved manufacturing processes have reduced PMD of single mode fibers down to 0.02–0.05 ps/$\sqrt{\text{km}}$, this performance is guaranteed only when the fiber is well protected against deformations and external forces, e.g., in a loose-tube cable. Situation is different, when the fiber has thick, tightly applied polymeric protective buffer. Forces transferred from such buffer to fiber are non-negligible and depend strongly on operating temperature because of mismatch between thermal expansion coefficients of silica and polymers. Buffer material, method of buffer application and variations in polymer crystalline phase content all have considerable influence here.

An important, but mostly neglected factor is the presence of circular strain in the fiber core, introduced either by stranding of cable components or fiber spinning during drawing. Such strain, if large enough, can dramatically improve stability of PMD in a fiber being subject to mechanical disturbances and variable temperatures.

Experiments described in previous paper on the same subject, presented in *Journal of Telecommunications and Information Technology*, no. 3, 2005 [1] and elsewhere [2, 3] revealed strong increase of PMD in most – but not all tight-buffered fibers at low temperatures. This paper covers:

- additional experiments on fibers and cables;
- fiber-buffer interactions and resulting PMD changes;
- influence of fiber twisting and spinning on PMD stability.

Some test data are presented in report [4]. Detailed descriptions and analysis are included in Ph.D. thesis by the same author [5].

2. Experiments

2.1. PMD measurement setup

Both the procedure for testing temperature-induced effects in optical fibers and instruments used at National Institute of Telecommunications (NIT) were presented in [1]. A new PMD measurement setup (Figs. 1 and 2), still based on

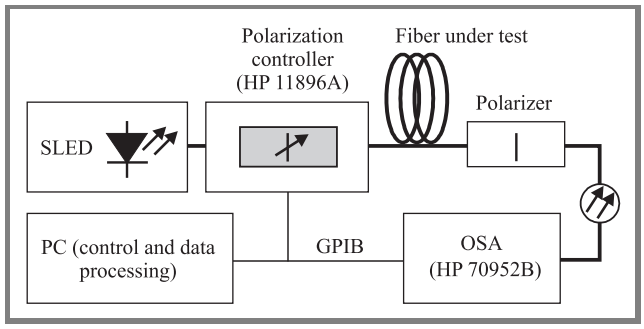

Fig. 1. Block diagram of PMD measurement setup with SLED source.

the fixed analyzer method [6] was introduced. Use of superluminescent light emitting diode (SLED) source and optical spectrum analyzer (OSA) reduced measurement time, extended spectral range to 1250–1650 nm and improved resolution to 0.01 ps. Instruments were controlled by a personal computer (PC) through the general purpose interface bus (GPIB).

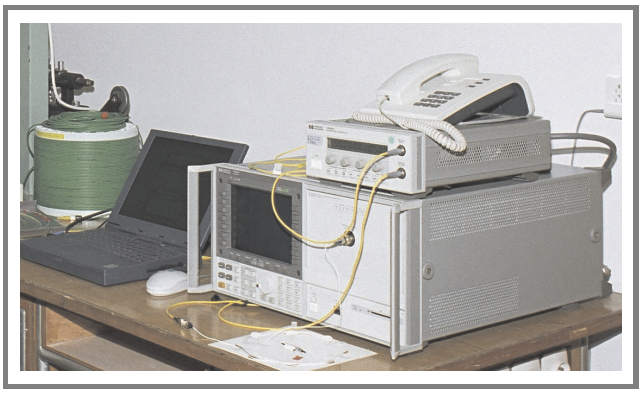

Fig. 2. PMD measurement setup: laptop PC (left), polarization controller (upper right), OSA (right), polarizer with connectors (bottom). SLED source not shown.

2.2. Preparation of samples

To minimize PMD variations due to pressure between layers of fiber or cable, several samples under test have been loosely hanged on a supporting tube or coiled on a flat plate rather than wound on a spool or drum (see Fig. 3). This ensures a more realistic approximation of operating conditions.

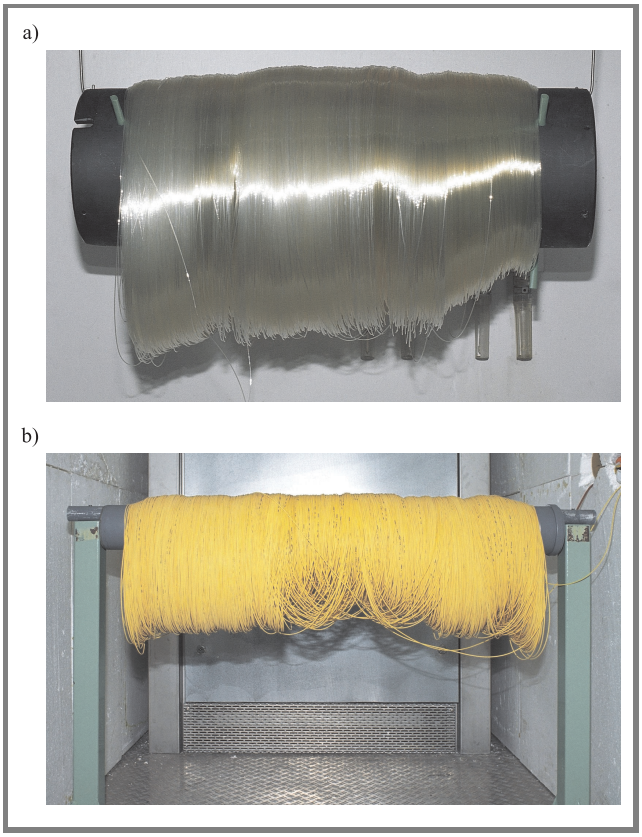

Fig. 3. Samples of tight-buffered fiber (a) and indoor cable (b) in the environmental chamber.

Cables with loose tubes effectively protecting the fibers from external crush forces were tested on standard drums. Care was taken to minimize fiber movements, in particular vibrations and dancing caused by forced air flow inside the environmental chamber. Fibers suspended in the air were particularly prone to such disturbances, resulting in random bending and fluctuations of state of polarization. This in turn produced rapid variations in spectra recorded during PMD measurements (Fig. 4).

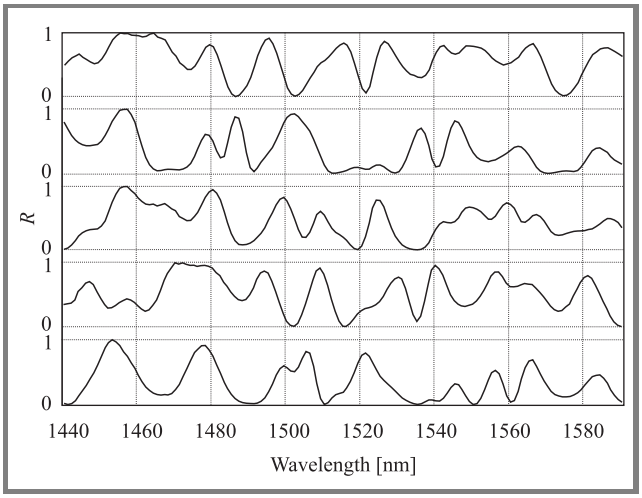

Fig. 4. Transmission spectra $R(\lambda)$ acquired during 5 fixed analyzer scans at 5 min intervals. Single mode fiber (SMF) in 0.9 mm semi-tight buffer, 6177 m long. Forced air circulation. The fiber was hanging loosely and air flow caused dancing.

Without forced air movement, transmission spectra variations in fixed temperature regime were smaller and occurred gradually (Fig. 5), primarily due to slowly changing temperature of the sample. This, however, did not reduce variability of PMD results in successive measurements. In fact, minor mechanical and thermal disturbances to fiber under test are believed to improve accuracy of PMD measurement, as they ensure collection of wider and more representative set of test data [7].

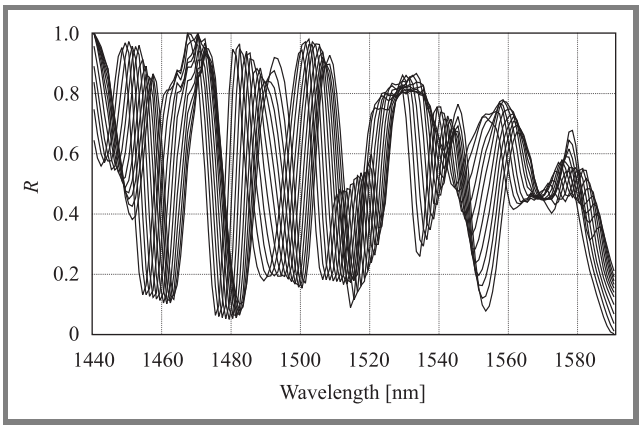

Fig. 5. Twelve transmission spectra $R(\lambda)$ acquired at 5 min intervals. Sample temperature rose by approximately 1°C during this time. Sample as in Fig. 4. Air circulation was switched off.

Uncertainty of PMD measurements was reduced by averaging 6–20 results obtained at each temperature. No significant change in fiber attenuation was observed during any experiment presented here.

2.3. PMD-temperature characteristics: tight-buffered fibers

2.3.1. Indoor cable with G.652 fiber

This cable (Tele-Fonika W-NOTKSd 1J 2,0) had a single non dispersion-shifted (SMF, ITU-T G.652) [8] fiber in a 0.9 mm extruded poly-butylene-terephtalate (PBT) tight buffer, aramide strength member, low smoke zero halogen (LSZH) jacket and diameter of 2 mm. The sample (Fig. 3) was 4040 m long.

Previous test on this cable [1] revealed rise of PMD at temperatures below 0°C, and large, permanent increase of PMD after cooling from +60°C to room temperature. This effect was attributed to increase of content of crystalline phase and related shrinkage of PBT buffer.

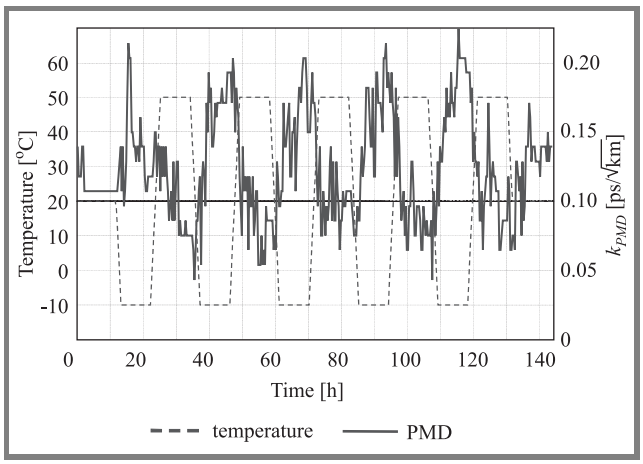

Fig. 6. Changes to PMD coefficient (k_{PMD}) of G.652 fiber in extruded buffer during temperature cycling test no. 1.

To investigate this issue further, the cable was initially subjected to 5 temperature cycles between –10°C and +50°C, with a controlled rate of 20°C/h, and dwell time of 9 h. Figure 6 shows the results.

Conclusions and observations were as follows:

- There was a small increase of PMD in each cycle and at all temperatures.
- Dwell time was too short for complete stabilization of PMD, so the results are not accurate.

In the next test, the same cable was subjected to 3 temperature cycles, with temperature range extended to –20°C...+60°C and rate of change 20°C/h. Dwell time was increased to 24 h, in order to ensure full stabilization of PMD. Results are shown in Fig. 7.

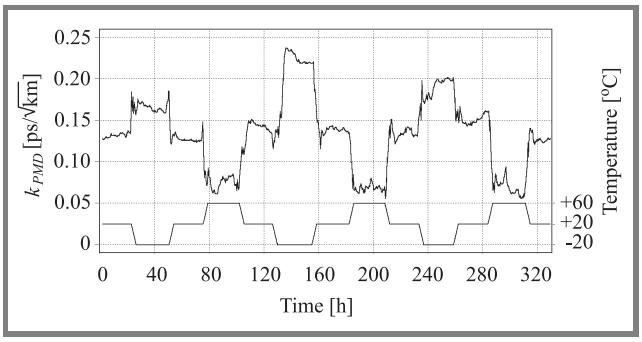

Fig. 7. Variations of PMD coefficient of indoor cable with G.652 fiber in extruded buffer during temperature cycling test no. 2. Lower graph shows temperature profile.

Conclusions and observations after this test:

- Large variations of PMD between temperature cycles.
- Thermal history has most effect on PMD at –20°C, and none at +60°C. This is due to reduction of forces acting on the fiber at high temperature and "reset" of polymer condition when the glass transition temperature T_g (approx. +50°C for PBT) is exceeded (see Subsections 3.2–3.4).
- Reduction of PMD in the last cycle proves the observed process is reversible, ruling out polymer oxidation, decomposition, cracking, etc. Variations in crystalline phase content due to differences in cooling conditions in each cycle are the most likely reason for effects observed.

2.3.2. Tight-buffered G.652 fiber

This test was preformed on 460 m long fiber with a 0.9 mm extruded polyamide tight buffer, made by Sumitomo (Japan). The experiment was carried out during COST-291 short-term scientific mission (STSM) [4]. Figure 8 shows the PMD characteristics in thermal equilibrium conditions.

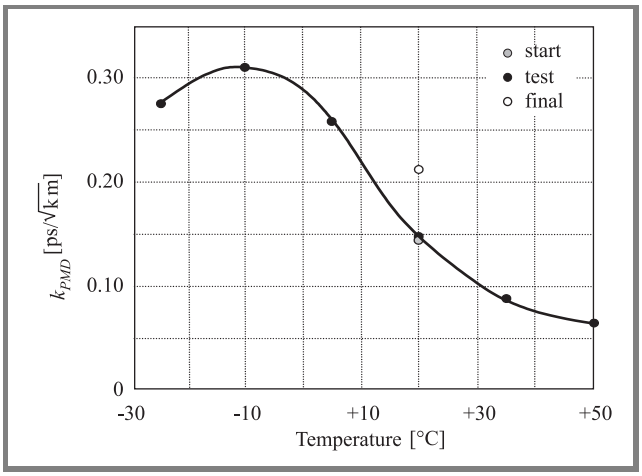

Fig. 8. PMD-temperature characteristics of G.652 fiber in nylon buffer. Steady-state data.

The following effects have been detected:

- Strong rise of PMD with decrease of temperature, but this effect is reversed below –10°C.
- Thermally induced component of PMD has exceeded 0.30 ps/$\sqrt{\text{km}}$ at –10°C.
- Permanent increase of PMD after test, probably due to crystallization and shrinkage of polyamide.

A graph plotted using all data (Fig. 9) shows strong PMD transients. There was always a temporary change of PMD

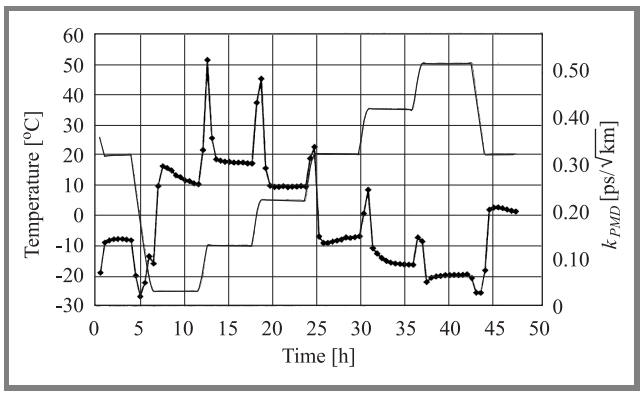

Fig. 9. Fiber PMD coefficient (bold line) and temperature (thin line) during temperature cycling of G.652 fiber in tight nylon buffer. PMD transients at each temperature transition are well visible.

in a direction **opposite** to what was observed in steady-state condition. This is likely due to finite time necessary for relaxation of coating and buffer polymers and reduction of internal strains.

2.3.3. Indoor cable with G.655 fiber

Cable selected for this test (TP SA OTO Lublin, Poland, W-NOTKSdD 1J5 2,0) had a single nonzero dispersion-shifted (NZDSF, ITU-T G.655) [9] fiber in a 0.9 mm UV-cured acrylate buffer, aramide strength member, low-smoke zero halogen jacket and external diameter of 2 mm. It was 4083 m long. Test results are presented in Fig. 10.

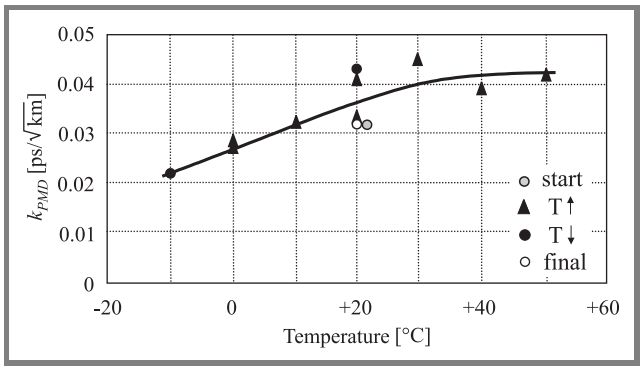

Fig. 10. PMD-temperature characteristics of indoor cable with G.655 fiber in UV-cured buffer.

This sample exhibited very interesting behavior:

- **Reduction** of PMD at temperatures below +20°C. This is opposed to **increase** of PMD in identical cable with G.652 fiber [1]; the difference must be due to special properties of G.655 fiber.
- No permanent increase of PMD. The buffer is made of cross-linked material with good dimensional stability.

2.3.4. Tight-buffered optical unit with stranded G.652 fibers

The test was performed on 170 m long 12-fiber optical unit extracted from optical ground wire (OPGW) made by AFL Telecommunications (USA). Design of this OPGW and its optical unit were presented in paper [1]. Fibers are stranded helically around a rigid strength member with a 125 mm pitch. For the test, all fibers were fusion spliced together, giving a total length of 2040 m.
OPGWs used in overhead high voltage lines have wide range of operating temperatures: –40…+85°C, so test conditions were chosen accordingly. This test was performed during COST-291 STSM [4].
Figure 11 shows results collected in steady-state conditions; transient data have been deleted.

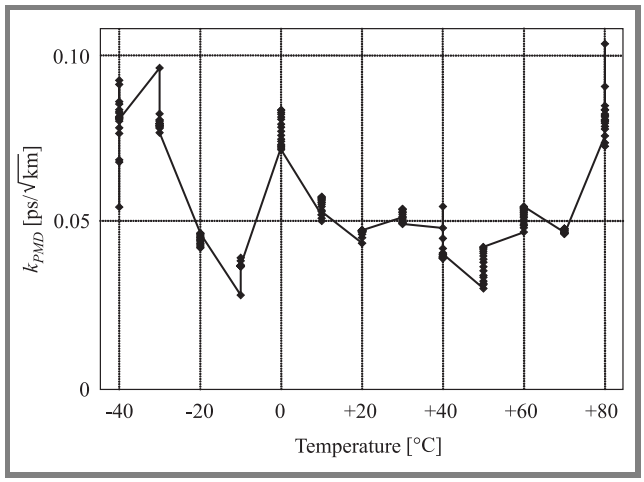

Fig. 11. PMD-temperature characteristics of tight-buffered OPGW unit with stranded G.652 fibers.

This sample has shown remarkable stability of PMD over a wide range of temperatures; some increase occurred only at **both** extreme temperatures: –40°C and +80°C. Most measured PMD values were close to 0.05 ps/$\sqrt{\text{km}}$.

2.4. PMD-temperature characteristics: loose tube cable

This was an optical ground wire with gel-filled central loose tube (Fig. 12) holding 24 loose optical fibers of non dispersion-shifted type (ITU-T G.652). Large space for movement of fibers minimize strain, bending and external pressure.

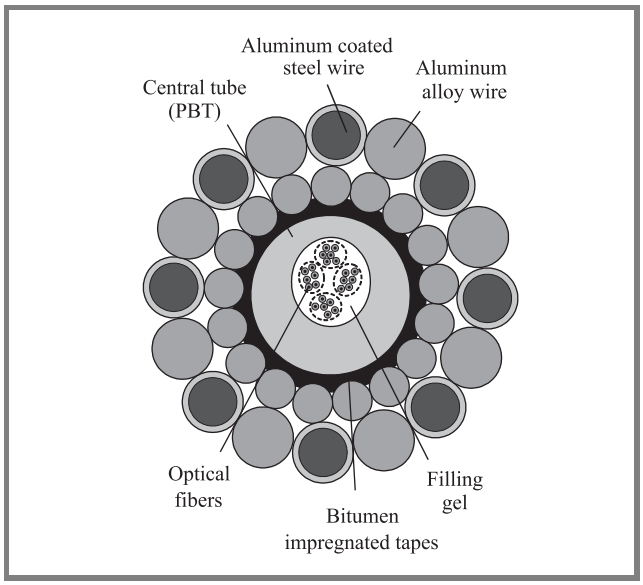

Fig. 12. Cross-section of loose-tube OPGW (NK Cables AACSR/AW SS-24F 64/34).

All 24 fibers in the 1310 m long OPGW were fusion spliced together, having a total length of 31.7 km. As seen on Fig. 13, there was little variation of fibers' PMD with

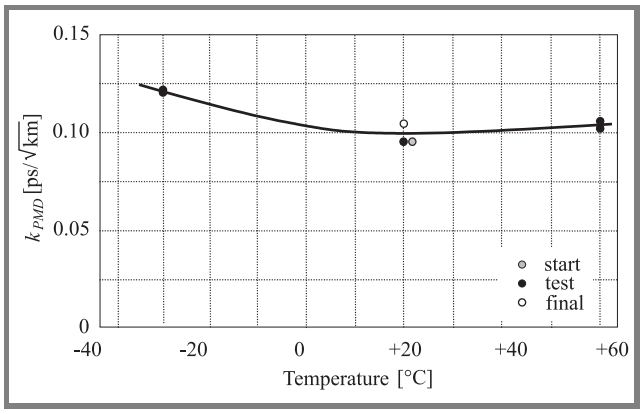

Fig. 13. PMD-temperature characteristics of loose-tube OPGW with G.652 fibers.

temperature and no permanent increase after test. This confirms assumption that forces generated by shrinking or expanding tight buffer are primarily responsible for PMD instability observed in several other samples.

2.5. Strain-temperature characteristics: tight-buffered fibers

Temperature-induced changes in axial fiber strain were measured for two indoor cables, each with a single fiber having a 0.25 mm primary coating and 0.9 mm tight buffer:

A) Tele-Fonika W-NOTKSd 1J 2,0; fiber buffer was extruded of PBT;

B) OTO Lublin W-NOTKSdD 1J5 2,0; fiber buffer was made of UV-cured acrylate.

Both cables were subjected to temperatures from –20°C to +50°C and optical length of fibers was measured with optical time domain reflectometer (OTDR). Sample lengths were 4040 m (A) and 4083 m (B). OTDR measurements were performed at 1310 nm and 1550 nm wavelengths. Figure 14 shows variations in fiber length relative to reference measurements at +20°C. Results obtained at both wavelengths were averaged and corrected for elastooptic effect with a factor of 1.25.

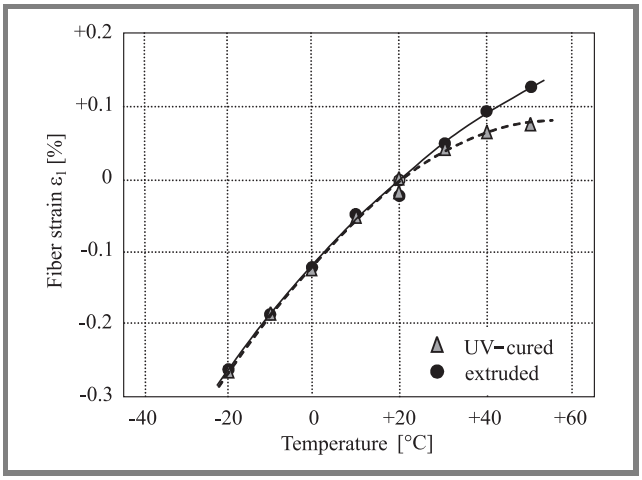

Fig. 14. Relative axial strain versus temperature: fibers in extruded and UV-cured 0.9 mm tight buffers.

Thermal expansion coefficients of both fibers at low temperatures are similar, about $7.5 \cdot 10^{-5}$/K at –10°C. However, fiber B has much lower zero-strain temperature (T_R), at which the strain approaches zero. Estimated T_R of this fiber is +60°C. Estimated T_R of fiber A in extruded buffer exceeds +100°C.

Lower T_R means smaller absolute compressive strain in fiber B – estimated to be 0.28% at the lowest operating temperature of –10°C, reduced tendency to buckling plus superior stability of PMD and attenuation. On the other hand, this fiber is also less tolerant to elongation caused by tensile forces.

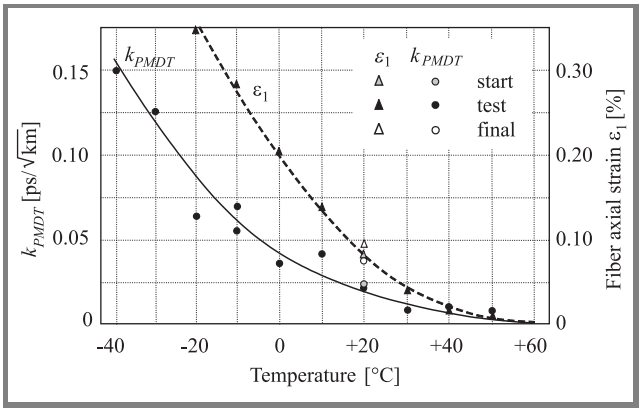

Fig. 15. Fiber strain (ε_1) and coefficient of thermally induced PMD (k_{PMDT}) in a G.652 fiber caused by shrinkage of 0.9 mm UV-cured acrylate buffer.

Data from this test allowed to analyze results of tests on PMD temperature dependence in a cable identical with "B", but containing a G.652 (unspun) fiber, presented earlier in paper [1]. Figure 15 shows a comparison between temperature dependence of fiber axial (compressive) strain and thermally induced PMD component. It is evident that induced PMD is roughly proportional to fiber strain.

3. Thermal and mechanical properties of fiber in tight buffer

3.1. Design and manufacturing of tight buffer

Typical tight-buffered fiber used in indoor, "universal" and some military cables is shown in Fig. 16. A thick layer of hard polymer is added over a standard primary coated fiber to make it stronger and easier to handle, especially when fitting optical connectors. Some buffer designs involve two layers: soft inner one, e.g., made of silicone and hard outer one, e.g., made of nylon.

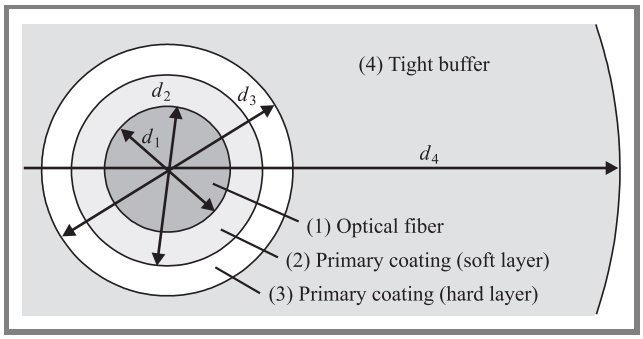

Fig. 16. Cross-section and dimensions of fiber in a typical 0.9 mm tight buffer.

Typical dimensions of buffered fiber for indoor cables and material data are listed in Table 1. Comparison of those data clearly indicates that it is the tight buffer, whose properties dictate mechanical forces acting on the glass fiber in variable temperatures; contribution from primary coating is marginal.

Tight buffers are applied to fibers using two methods:

1) extrusion of polymer, most often PBT, PVC or nylon – predominantly PA12 and its blends (Fig. 17);

2) UV-curing of liquid acrylate compounds on the fiber.

Commonly used extrusion process requires temperature of approximately +250°C. Melted polymer is usually rapidly cooled with cold water, in order to limit crystallization of PBT or polyamide and post-extrusion shrinkage. The partially ordered crystalline phase has a density approximately 2% higher than amorphous one [10], so this approach reduces undesirable buffer shrinkage and fiber strain. However, operation of fiber above the glass transition temperature of polymer (T_g), being about +40...+60°C for PBT and PA12, and subsequent slow cooling causes crystalline phase content to increase and the buffer to shrink further. This shrinkage may be reversed by heating above T_g again and rapid cooling, but results of such treatment are hardly predictable, as presented in Subsection 2.3.1. This problem is absent in cured and amorphous polymers.

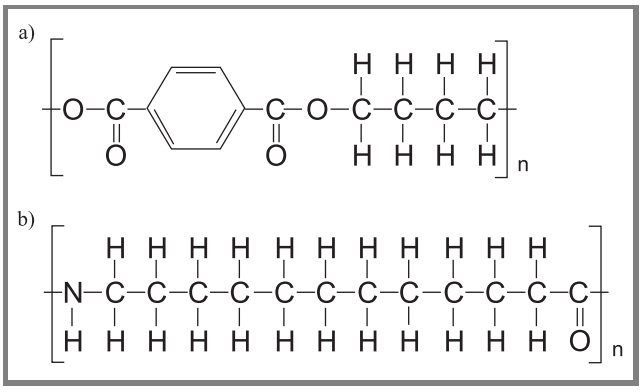

Fig. 17. Structures of common buffer materials: PBT (a) and PA12 (b).

Table 1

Thermo-mechanical data of Corning SMF-28 fiber in extruded PBT tight buffer at +20°C; layer numbering in accordance with Fig. 16

No.	Component (layer) of buffered optical fiber	Young modulus (E)	External diameter (d)	Cross-section	Thermal expansion coefficient (α)
		[MPa]	[mm]	[mm^2]	[K^{-1}]
1	Silica glass fiber	73000	0.125	0.0123	$5.5 \cdot 10^{-7}$
2	Soft primary coating	1.4	0.190	0.0161	$2.2 \cdot 10^{-4}$
3	Hard primary coating	700	0.250	0.0207	$8.0 \cdot 10^{-5}$
4	Tight buffer (PBT)	2500	0.900	0.5871	$1.3 \cdot 10^{-4}$

Buffered fiber is subject to axial compressive strain of 0.05–0.35% at room temperature, with zero stress temperature (T_R) between +50°C and +190°C [5]. This strain can be reduced if a suitable tension is applied to fiber during application of a buffer.

Curing of liquid material with ultraviolet light is in theory a "cold" process, but intense radiation required for high-speed curing can heat the fiber up to 100°C, and subsequent shrinkage is increased. Nevertheless, UV-cured buffer generally produces less strain on the fiber (see Subsection 2.5) and its circularity is better.

3.2. Temperature-dependent axial strain

Axial fiber strain increases with falling temperature due to contraction and rise of modulus of buffer material, according to simplified formula [5]:

$$\varepsilon_1 = \frac{\left(d_4^2 - d_3^2\right)E_4}{d_1^2 E_1 + \left(d_4^2 - d_3^2\right)E_4} \int_T^{T_R} (\alpha_4 - \alpha_1) dT$$

$$\approx \frac{\left(d_4^2 - d_3^2\right)E_4}{d_1^2 E_1 + \left(d_4^2 - d_3^2\right)E_4} (T_R - T)\, \alpha_{4eff}\,, \qquad (1)$$

where: ε_1 is fiber strain, T – operating temperature, T_R – zero stress temperature, d_4, d_3 – outer and inner diameter of hard buffer (Fig. 16), α_1, α_4 – thermal expansion coefficients of silica and buffer material, E_1, E_4 – Young moduli of silica and buffer, α_{4eff} – effective thermal expansion coefficient of buffer material between T and T_R.

Beginning from zero level at T_R, compressive strain increases with decrease of temperature, as shown in Figs. 14 and 15. Pure axial strain does not produce difference between refractive indices for polarization modes in the fiber core, so it doesn't affect fiber PMD.

3.3. Lateral strain

Internal strain in the fiber in the direction perpendicular to its axis produces a mechanically induced optical birefringence M and differential group delay $\Delta\tau$ in accordance with formulae below:

$$M = n_x - n_y = R(\sigma_x - \sigma_y)\,, \qquad (2)$$

$$\Delta\tau = \frac{[R]L}{c}(\sigma_x - \sigma_y)\,, \qquad (3)$$

where: M – mechanically induced birefringence, n_x, n_y – refractive indices in x and y directions, σ_x, σ_y – strains in x and y directions, R – the elastooptic coefficient, equal to $-3.15 \cdot 10^{-6}$/MPa for SiO_2 glass at 1550 nm, L – fiber length.

The coefficient of polarization mode dispersion component mechanically induced in a long fiber with uniform strain distribution is described by the formula:

$$k_{PMDM} = \frac{R}{c}\sqrt{\frac{h}{1000}}(\sigma_x - \sigma_y)\,, \qquad (4)$$

where: c – speed of light in vacuum, h – coupling length of polarization modes [m].

For a typical $h = 10$ m, a 1 MPa lateral differential strain produces PMD as high as 1.05 ps/$\sqrt{\text{km}}$.

In general, lateral strain is proportional to axial strain, as both result from polymer shrinkage. The latter is easier to measure, however – see Subsection 2.5.

At room temperature, the uneven lateral shrinkage or ellipticity of buffer affects the fiber relatively little, because the soft inner layer of coating prevents transfer of any significant pressure to glass fiber. This protection disappears below glass transition temperature (T_g) of coating, when it stiffens. Depending on particular material of primary coating, its T_g can be between 0°C and –80°C (see Fig. 18).

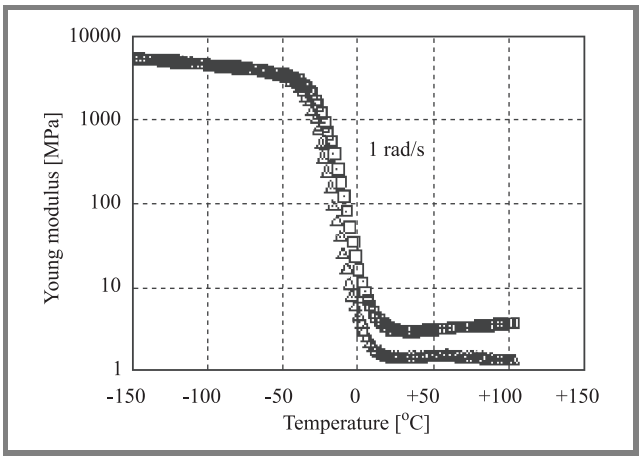

Fig. 18. Temperature dependence of modulus for two UV-cured acrylate compounds used for soft primary coatings [11].

When the buffer lacks perfect circularity, mechanically induced PMD appears and quickly grows at low temperatures approaching T_g of primary coating. This process is augmented by buffer shrinkage. However, it is possible that further cooling causes increased mixing of polarization modes due to unevenly distributed pressure, resulting in saturation of PMD growth or even some reduction of PMD, as presented in Subsection 2.3.2.

3.4. Fiber bending and buckling

Eccentricity of coating and buffer results in non-symmetry of longitudinal forces due to polymer shrinkage, causing fiber bending; bend curvature rises with falling temperature. Deformation of fiber produces mechanical strains and induces PMD in accordance with Ulrich formula [12]:

$$k_{PMDB} = \frac{k}{r_B^2}\,, \qquad (5)$$

where: k_{PMDB} – the bending-induced PMD coefficient [ps/$\sqrt{\text{km}}$], k – proportionality factor, being 200–3500 ps·mm^2/$\sqrt{\text{km}}$ for G.652 fibers [5], r_B – fiber bending radius.

Excessive axial strain leads to fiber **buckling**: loss of mechanical stability and deformation of fiber into a helix or wave pattern. With a high quality buffer this process occurs suddenly at critical low temperature, in order of –40°C, causing abrupt increase of fiber loss and PMD.

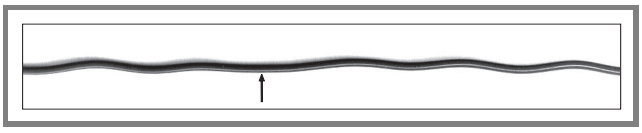

Fig. 19. Buckled fiber in a 0.9 mm buffer. The fiber has formed a reversible spiral, with arrow showing a reversal point. The image is shortened by a factor of 1:4 for better visibility.

If the buffer has frequent imperfections producing minute fiber bends, the latter grow gradually with decreasing temperature. In a bad quality product, buckling can occur even at room temperature, with distinct deformation and helix diameter up to 3 mm (see Fig. 19). Embedding of fiber in a cable severely restricts such deformation.

Helically deformed fiber moves inside soft coating and is pressed against the hard coating above. At the same time, a formerly rigid, straight fiber becomes a spring offering little resistance to axial shrinkage of polymeric buffer with decreasing temperature. Assuming that helix diameter is restricted by buffer size and cable design to a certain value d_{TS} (usually 0.1–1 mm), fiber bending radius can be estimated as

$$r_B = \frac{d_{TS}}{4\alpha_4 \cdot (T_B - T)} + \frac{d_{TS}}{2}, \tag{6}$$

where: T_B is the critical buckling temperature, and T – operating temperature.

Substituting formula [5] into [6], one can estimate the PMD resulting from such a temperature-dependent bending:

$$k_{PMDT} \approx \frac{16k \cdot \alpha_4^2 \cdot (T_B - T)^2}{d_{TS}^2}. \tag{7}$$

It must be noted, however, that a high quality buffered fiber shall **not** experience any significant buckling over the full range of specified operating temperatures. This still leaves the induction of PMD due to lateral strain, however.

Equation (7) explains why several manufacturers of industrial and military-grade cables have adopted 2-layer buffers, usually of 0.4/0.9 or 0.5/0.9 mm size: a soft inner layer of material like silicone allows to increase d_{TS} to 0.4–0.5 mm, dramatically reducing detrimental fiber bending at low temperatures.

Total PMD induced in the fiber due to mechanical influence of tight buffer shrinking with decrease of temperature can be estimated using a simplified, semi-empirical formula:

$$k_{PMDT} = k_1(T_1 - T)^2 + k_2(T_2 - T), \tag{8}$$

where: k_{PMDT} – PMD coefficient resulting from thermal contraction of buffer and coating, k_1, k_2 – proportionality factors, T_1, T_2 – threshold temperatures.

Data obtained during temperature cycling tests of tight-buffered, un-spun single-mode fibers presented in paper [1] and here (see Figs. 8 and 15) confirm applicability of formula (8).

Fibers in indoor and field deployable cables sometimes have a "semi-tight" buffer – extruded loose tube of 0.9 mm diameter with a single fiber surrounded by a layer of gel some 0.05–0.10 mm thick. Unlike tight designs, the buffer is not mechanically bonded to fiber, so its extrusion shrinkage and thermal expansion are about twice as large in comparison to tight buffer. Unless considerable tension is applied during extrusion, fiber often suffers from excessive overlength and has high PMD due to bending and pressure against buffer walls, even across a full range of operating temperatures.

Total PMD coefficient of tight-buffered fiber at low temperature is given by the following formula:

$$k_{PMD} = \sqrt{k_{PMDG}^2 + k_{PMDT}^2}, \tag{9}$$

where: k_{PMDG} is the "natural" PMD coefficient dictated by non-perfect fiber geometry, close to what is measured in a primary coated fiber at room temperature.

Contribution of thermo-mechanically induced PMD is noticeable only when it becomes comparable to "natural" PMD of a particular fiber, therefore high PMD fibers tend to exhibit superior PMD stability than low PMD ones, which need better mechanical protection to retain their properties.

4. Effects of fiber spinning and stranding on PMD

4.1. Spun fibers

Introduction of dispersion-shifted and nonzero-dispersion shifted single mode fibers (ITU-T G.653 and G.655) [9], characterized by smaller core size and increased doping levels with respect to standard non dispersion-shifted fiber (ITU-T G.652) has created difficulties with ensuring perfect fiber geometry and low PMD, especially as demands of customers kept growing. An elegant and almost universally adopted solution is "spinning" of fiber – rotation at constant or modulated rate, applied to fiber during drawing from a hot preform [13], first introduced to mass production of telecom fibers by AT&T in 1993. Semi-molten glass drawn from the tip of the preform is easily and permanently deformed. Spinning prevents accumulation of birefringence in a fiber drawn from preform with non-circular core, as this deformation is regularly rotated in different locations along the fiber and their individual contributions to birefringence cancel each other. Spinning, in fact, has been originally applied to make low-birefringence sensor fibers back in 1979 [14].

The simpler non dispersion-shifted fibers have largely continued to be drawn without spinning, albeit the process is becoming more common since 2005.

4.2. Stranding of optical units

Stranding of multiple units to form a cable or its core is a common process in the cable industry, extensively used in manufacturing of optical fiber cables. As no untwisting is usually applied later, this step leaves a permanent circular strain in the parts being stranded. This is normally not an issue with copper wires, aramide yarns or plastic parts, e.g., loose tubes in optical fiber cable.

While fibers inside stranded tubes can move and relax – especially when stranding is of reversible type, stranding of fibers to form a tight-buffered multi-fiber unit leaves a permanent strain, as any fiber movement is prevented by rigid coatings and buffers holding fibers and other parts together. The same can happed in a multi-fiber indoor cable, where fiber units have common sheath and yarn filling. As typical rates of twist do not affect fiber reliability or attenuation, this effect is usually ignored.

4.3. Circular strain and fiber PMD

Twisting of optical fiber creates circular strain and related circular birefringence, meaning a rotation of light polarization plane with rate proportional to fiber twist rate γ:

$$\delta = 2\pi g_s \gamma z = 2\pi \frac{g_s}{\Lambda_S} z, \tag{10}$$

where: δ – rotation angle of polarization plane, g_s – stress-optic rotation coefficient of optical fiber, γ – fiber twist rate [rev/m], Λ_S - stranding pitch [m], z – distance from the beginning of twisted fiber section.

The stress-optic rotation coefficient is defined by the following equation:

$$g_s = \frac{E_{SF} \cdot R}{n_2}, \tag{11}$$

where: E_{SF} – modulus of rigidity (shear modulus) of fiber core material, n_2 – refractive index of fiber core.

Substituting the following parameters of single-mode silica fiber operating at 1550 nm: $E_{SF} = 31000$ MPa, $R = -3.15 \cdot 10^{-6}$/MPa and $n_2 = 1.47$, one obtains $g_s = 0.0665$. Measurements of single mode telecom fibers give $g_s \approx 0.07$ [19, 20].

Fiber twisting produces two circular polarization modes with opposite rotation directions and circular birefringence [16], causing a differential group delay $\Delta\tau$ and twist-induced PMD (k_{SPMD}). For uniform twist, their values can be calculated as follows [5]:

$$\Delta\tau = 0.065 \gamma L, \tag{12}$$

$$k_{SPMD} = 0.065 \sqrt{\frac{h}{1000}}. \tag{13}$$

In the formulae above, h is expressed in [m], $\Delta\tau$ in [ps], and the PMD coefficient k_{SPMD} in [ps/$\sqrt{\text{km}}$].

Assuming a typical coupling length $h = 10$ m, fiber twisting at 8 rev/m rate, measured for the 12-fiber tight buffered optical unit of OPGW tested in our lab produces PMD with $k_{SPMD} = 0.052$ ps/$\sqrt{\text{km}}$. This corresponds pretty well to surprisingly repeatable PMD values measured in several experiments on this type of OPGW and optical unit extracted from it (see [1] and Subsection 2.3.4).

Besides generation of PMD by twisting, excellent stability of PMD suggests there is additional mechanism present in twisted fibers, capable of reducing PMD contributions resulting from mechanical influences presented in Section 3.

Periodic rotation of polarization plane prevents accumulation of $\Delta\tau$ in a fiber being subject to perpendicular mechanical stress with a (relatively) fixed direction, because locally generated contribution to birefringence experiences "modulation" and change of sign with respect to birefringence accumulated in the preceding length of fiber. The resulting reduction of mechanically-induced PMD is described by the following PMD reduction factor [5]:

$$\zeta_S \approx \frac{1}{\sqrt{1 + 0.0196\left(\frac{L_B}{\Lambda_S}\right)^2 + 0.0182\left(\frac{L_B}{\Lambda_S}\right)^4}}, \tag{14}$$

where: L_B – fiber beat length [m].

With a relatively strong twist, when $L_B/\Lambda_S \geq 5$, the PMD reduction factor is approximately proportional to square of the L_B/Λ_S ratio:

$$\zeta_S \approx 7.4\left(\frac{\Lambda_S}{L_B}\right)^2. \tag{15}$$

For the majority of telecom type single mode fibers, characterized by $L_B \geq 5$ m, a 100-fold reduction of PMD generated by external crush forces ($\zeta_S = 0.01$) can be ensured by twisting the fiber with a $\Lambda_S = 183$ mm pitch; this corresponds to a twist rate $\gamma = 5.44$ rev/m.

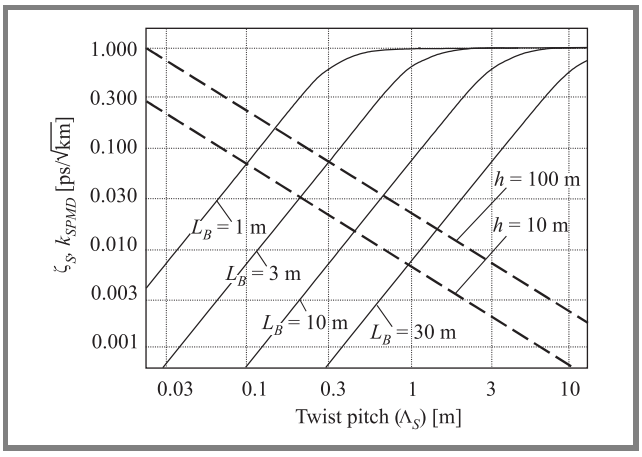

Fig. 20. Characteristics of PMD reduction factor, applicable to PMD induced by fixed direction crush forces (ζ_S) (continuous lines) and PMD introduced by twisting in a nonzero dispersion-shifted fiber (k_{SPMD})($\lambda = 1550$ nm, dashed lines) versus fiber twist pitch.

Characteristics of PMD reduction factor and twist-generated polarization mode dispersion are plotted in Fig. 20. One shall notice, that excessive twisting, besides possible problems with mechanical design and reliability of optical fiber cable, can easily produce PMD high enough to severely degrade transmission performance of fiber, negating the beneficial effects of improved tolerance to bending and external forces.

It was also necessary to explain the apparently odd results obtained during low-temperature tests on tight-buffered nonzero dispersion-shifted fibers (NZDSF, ITU-T G.655), presented in Subsection 2.3.3 and paper [1]. Those fibers were not twisted, but still exhibited greatly superior resistance to mechanical induction of PMD in comparison to standard single-mode fibers (SMF, ITU-T G.652) operating in comparable conditions.

As indicated in Subsection 4.1, the difference lies in spinning of G.655 fibers. A by-product of this process is the presence of residual circular strain in the spun fiber, as the fiber cannot fully relax once it is colder and its glass becomes more viscous when leaving the melting zone.

Measurements of unidirectionally spun G.652 fibers [17] suggest that residual strain corresponds roughly to twisting of fiber at a rate equal to 10% of spinning rate. For a typical spinning rate of 5 rev/m, we get $\Lambda_S = 2$ m, which (see Fig. 20) provides at least a 10-fold reduction of mechanically induced PMD in a good quality fiber with $L_B \geq 20$ m. This explains superior stability of PMD in (spun) G.655 fibers in comparison to (unspun) G.652 fibers we have tested.

5. Conclusions

Both laboratory experiments and theoretical analysis have clearly proved that single-mode fibers placed in thick "tight" or "semi-tight" polymeric buffers of type commonly used in optical fiber cables can be susceptible to detrimental mechanical forces generated by the buffer, particularly at low temperatures. While fiber attenuation is usually not affected, its polarization mode dispersion in cold environment can increase dramatically, by up to 0.3 ps/$\sqrt{\text{km}}$ and even more. This effect has so far been overlooked by researchers and engineers responsible for cable and system specifications.

While harmful to operation of high-speed networks, this phenomenon can be used in research and diagnostics of optical fiber cables.

Induction of PMD by forces exerted by fiber buffer can be eliminated or reduced, when the fiber is either appropriately twisted during cable manufacture or spun during drawing. While both processes have been introduced by the industry for other reasons, they have an unintended beneficial side effect.

In particular, use of spun single-mode fibers in cables of tight buffer design intended for use at low temperatures or being subject to severe crush and bending is strongly recommended.

Acknowledgements

Most research work presented here was performed within COST Action 270 "Reliability of Optical Components and Devices in Communications Systems and Networks", and financed by the Polish Government research grant no. 632/E-242/SPB/COST/T-11/DZ198/2003-2005. Additional test data were gathered during short-term scientific mission (STSM) to Politecnico di Torino and Instituto Superiore Mario Boella (ISMB), Turin, Italy, within COST Action 291 "Towards Digital Optical Networks". The author is grateful to ISMB researchers Silvio Abrate and Augustino Nespola for their valuable assistance.

References

[1] K. Borzycki, "Influence of temperature and aging on polarization mode dispersion of tight-buffered optical fibers and cables", *J. Telecommun. Inform. Technol.*, no. 3, pp. 96–104, 2005.

[2] K. Borzycki, "Temperature dependence of PMD in optical fibres and cables", in *Proc. ICTON 2005 Conf.*, Barcelona, Spain, 2005, vol. 1, paper Tu.C3.7, pp. 441–444.

[3] K. Borzycki, M. Jaworski, and M. Marciniak, "Temperature dependence of PMD in tight buffered G.652 and G.655 single-mode fibers", in *Proc. OC&I-2006/NOC-2006 Conf.*, Berlin, Germany, 2006, pp. 21–28.

[4] K. Borzycki, "Report on COST-291 short term scientific mission to Politecnico di Torino (Turin, Italy)", July 2005.

[5] K. Borzycki, "Wpływ temperatury na dyspersję polaryzacyjną (PMD) jednomodowych włókien światłowodowych w pokryciach ścisłych" (Influence of temperature on polarization mode dispersion (PMD) of single-mode tight-buffered fibers), Ph.D. thesis, Warsaw, National Institute of Telecommunications, March 2006 (in Polish).

[6] "Transmission media characteristics – Optical fibre cables: Definitions and test methods for statistical and non-linear related attributes of single-mode fibre and cable", ITU-T Rec. G.650.2 (01/2005).

[7] A. F. Judy, A. H. McCurdy, R. K. Boncek, and S. K. Kakar, "Fiber PMD – room for improvement", in *Proc. NFOEC 2003 Conf.*, Orlando, USA, 2003, pp. 1208–1217.

[8] "Transmission media characteristics – Optical fibre cables: Characteristics of a single-mode optical fibre and cable", ITU-T Rec. G.652 (06/2005).

[9] "Transmission media characteristics – Optical fibre cables: Characteristics of a non-zero dispersion-shifted single-mode optical fibre and cable", ITU-T Rec. G.655 (03/2006).

[10] I. Gruin, *Materiały polimerowe*. Warszawa: Wydawnictwo Naukowe PWN, 2003 (in Polish).

[11] C. Aloisio, A. Hale, and K. Konstadinidis, "Optical fiber coating delamination using model coating materials", in *Proc. 51st IWCS Conf.*, Orlando, USA, 2002, pp. 738–747.

[12] R. Ulrich, S. C. Rashleigh, and W. Eickhoff, "Bending-induced birefringence in single-mode fibers", *Opt. Lett.*, vol. 5, no. 6, pp. 60–62, 1980.

[13] D. A. Nolan, X. Chen, and M.-J. Li, "Fibers with low polarization-mode dispersion", *J. Lightw. Technol.*, vol. 22, no. 4, pp. 1066–1077, 2004.

[14] S. R. Norman, D. N. Payne, and M. J. Adams, "Fabrication of single-mode fibres exhibiting extremely low polarisation birefringence", *Electron. Lett.*, vol. 15, no. 11, pp. 309–311, 1979.

[15] A. J. Barlow and D. N. Payne, "The stress-optic effect in optical fibers", *IEEE J. Quant. Electron.*, vol. QE-19, no. 5, pp. 834–839, 1983.

[16] T. Chartier, C. Greverie, L. Selle, L. Carlus, G. Bouquest, and L.-A. de Montmorillon, "Measurement of the stress-optic coefficient of single-mode fibers using a magneto-optic method", *Opt. Expr.*, vol. 11, no. 20, pp. 2561–2566, 2003.

[17] D. Sarchi and G. Roba, "PMD mitigation through constant spinning and twist control: experimental results", in *Proc. OFC'2003 Conf.*, Atlanta, USA, 2003, paper WJ2, pp. 367–368.

Krzysztof Borzycki was born in Warsaw, Poland, in 1959. He received the M.Sc. degree in electrical engineering from Warsaw University of Technology in 1982 and a Ph.D. degree in communications engineering from National Institute of Telecommunications (NIT), Warsaw in 2006. He has been with NIT since 1982, working on optical fiber fusion splicing, design of optical fiber transmission systems, measurement methods and test equipment for optical networks, as well as standardization and conformance testing of optical fiber cables, SDH equipment and DWDM systems. Other activities included being a lecturer and instructor in fiber optics and technical advisor to Polish fiber cable industry. He has also been with Ericsson AB research laboratories in Stockholm, Sweden, working on development and testing of DWDM systems for long-distance and metropolitan networks between 2001 and 2002 while on leave from NIT. He has been engaged in several European research projects since 2003, including Network of Excellence in Micro-Optics (NEMO) and COST Actions 270, 291 and 299. This included research on polarization mode dispersion in fibers and cables operating in extreme environments, and testing of specialty fibers. Another area of his work is use of optical fibers in electric power cables and networks. Dr. Borzycki is an author or co-author of 1 book, 2 Polish patents and over 40 scientific papers in the field of optical fiber communications, optical fibers and measurements in optical networks, as well as one of "Journal of Telecommunications and Information Technology" editors.

e-mail: k.borzycki@itl.waw.pl
National Institute of Telecommunications
Szachowa st 1
04-894 Warsaw, Poland